

PENDULAR TUNED MASS DAMPERS IN FREE-PLAN CHILEAN TALL BUILDINGS

René Zemp¹, Juan C. de la Llera², Leopoldo Breschi³

*1 M.Sc., Dept. of Struct. and Geotech. Engrg., Pontificia Universidad Católica de Chile. Santiago, Chile
currently Basler&Hofmann Consulting Engineers, Zürich, Switzerland*

*2 Professor, Dept. of Struct. and Geotech. Engrg., Pontificia Universidad Católica de Chile. Santiago, Chile,
3 Structural Engineer PUC, P.E., VMB, Santiago, Chile
Email: jllera@ing.puc.cl*

ABSTRACT :

The first low-cost tuned mass damper system in Chilean building construction was recently designed and included on a 21-story plus 6-basement building. The structure is an example of the so-called Chilean free-plan building concept, which is characterized by shear-wall elevator and staircase core plus a perimeter frame with shallow beams and post-tensioned reinforced-concrete slabs. This article focuses on the most relevant results of the design, construction, testing and implementation of a 150 kN magnetorheological (MR) damper developed to seismically control this structure equipped with 2 tuned masses (TMs) at the roof of 160 tons each. First, the governing non-linear equations of motion of the TM-MR damper assembly are presented. Building displacements and accelerations are computed and analyzed for a suite of subduction-type and near field ground motions. It is observed that the RMS response modification factors obtained for earthquake excitation are strongly dependent on the frequency content of the excitation and may range in the average from 9% to 37% relative to the bare structure. A complete testing program was performed on the constructed damper and a physical controller proposed for the MR damper. A pull-back test on one of the TMs in the building was carried out to validate this controller. Its performance is essentially equivalent to that of an LQR controller, but the information required to implement it is considerably less. The MR damper designed was capable of controlling the TM displacements very effectively.

KEYWORDS: TM-MR damper assembly, vibration control, free-plan building, tuned masses

1. INTRODUCTION

Building vibration induced by earthquake excitation may be reduced by the appropriate selection of a tuned inertial mass connected to a magneto rheological damper (TM-MR damper assembly). Several analytical studies have shown that by connecting a TM to a semi-active MR device in structures subjected to earthquake and wind excitation, it is possible to improve the building performance[4];[5]. MR-dampers are semi-active MR fluid devices that with very low power requirement are capable of changing a fluid from a free-flowing linear viscous state to a semi-solid state with controllable yield strength [3]. Due to this property, the reactive force applied on the TM exerted by the MR-damper can be dynamically controlled within a range.

This article shows first a comparison of the analytical earthquake and wind response of a TM-MR damper assembly built for a 21-story free-plan building in Santiago, Chile (Figure 1). Because the building is more flexible in the transverse direction (Y-direction) and presents some lateral torsional coupling, two pendular TMs, one along the flexible edge and one along the stiff edge of the building were designed and built (Figure 1). Each TM weighs approximately 160 ton, which represents in total 1.2% of the modal weight of the fundamental Y-direction mode $T=2.7s$ of the structure. Free small-amplitude vibration tests (3-4cm) on the TMs leads to essentially negligible TM damping ratios in the range of $\xi_p=0.1$ to 0.25%. Analytical results from an equivalent 2 DOF building model together with a full 3D nonlinear model of the TM-MR damper assembly were analyzed and compared. In this analytical part, a new physical control of the MR-damper force is proposed and compared with the well known LQR control strategy.

Then the article deals with the design, construction, testing, and implementation of the MR-damper in the R/C

building presented. Moreover, results presented are focused on the testing and implementation components of the research. An extensive testing program for the damper was carried out, including real-time hybrid simulations (HS). Most MR-damper modeling assumptions used in design were validated by these tests, including a model to analyze cavitation of the damper which is described elsewhere [6]. Finally, results from the pull-back tests performed on the flexible-edge TM, controlled by the physical controller, are described.

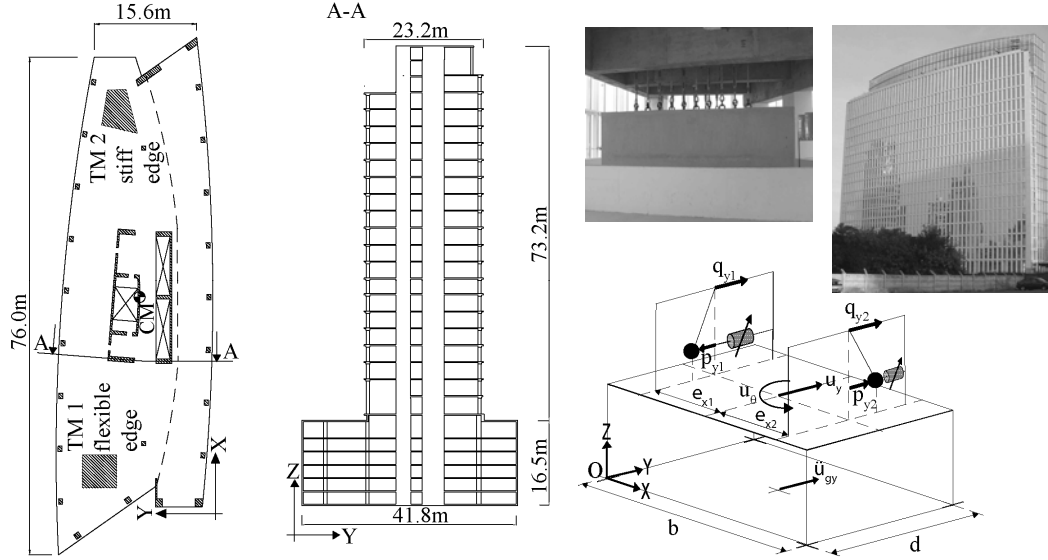


Figure 1 Building plan, elevation, TM, and approximate 2D model considered

2. SIMPLIFIED STRUCTURAL MODEL

A complete description of the 3D structural model of the building with the nonlinear TM-MR assembly is given elsewhere [1]. However, it can be shown that the equations of motion that govern the simplified system (used for predesign) shown in Figure 1 may be stated in parametric form as:

$$\begin{bmatrix} \mu_1(1+\beta)+1 & \frac{\mu_1}{b}(\beta e_{x2} - e_{x1}) & \mu_1 & -\beta\mu_1 \\ \frac{1+\alpha^2}{12\alpha^2} + \frac{\mu_1}{b^2}(e_{x1}^2 + \beta e_{x2}^2) & -\frac{\mu_1}{b}e_{x1} & -\frac{\mu_1}{b}\beta e_{x2} & \beta\mu_1 \\ \text{sym.} & \mu_1 & 0 & \beta\mu_1 \end{bmatrix} \begin{bmatrix} \ddot{u}_y \\ b\ddot{u}_\theta \\ \ddot{p}_{y1} \\ \ddot{p}_{y2} \end{bmatrix} + \begin{bmatrix} \frac{1}{M_1} \mathbf{BC} \\ \mathbf{0} \end{bmatrix} \begin{bmatrix} \dot{u}_y \\ b\dot{u}_\theta \\ \dot{p}_{y1} \\ \dot{p}_{y2} \end{bmatrix} + \begin{bmatrix} 0 & 0 \\ 2\xi_{p1}\omega_{p1}\mu_1 & 0 \\ 0 & 2\xi_{p2}\omega_{p2}\mu_1 \end{bmatrix} \begin{bmatrix} \dot{u}_y \\ b\dot{u}_\theta \\ \dot{p}_{y1} \\ \dot{p}_{y2} \end{bmatrix} + \omega_{oy}^2 \begin{bmatrix} 1 & \hat{e}_{sx} \\ \hat{e}_{sx} & \hat{e}_{sx}^2 + \frac{1+\alpha^2}{12\alpha^2}\Omega^2 \end{bmatrix} \begin{bmatrix} u_y \\ bu_\theta \\ p_{y1} \\ p_{y2} \end{bmatrix} + \begin{bmatrix} 0 \\ 0 \\ \frac{FTMD1}{M_1} \\ \frac{FTMD2}{M_1} \end{bmatrix} = - \begin{bmatrix} \mu_1(1+\beta)+1 \\ \frac{\mu_1}{b}(\beta e_{x2} - e_{x1}) \\ \mu_1 \\ \beta\mu_1 \end{bmatrix} \ddot{u}_{gy} \quad (2.1)$$

where the degrees of freedom $\mathbf{u} = [u_x \quad bu_\theta \quad p_{y1} \quad p_{y2}]^T$ are described in Figure 1 and consider the Y-direction translation and rotation of the building plan, and a single translation for each of the two inertial masses; $\Omega = \omega_{oy}/\omega_\theta$ is the uncoupled lateral-to-torsional frequency ratio; $\hat{e}_{sx} = e_{sx}/b$ is the normalized stiffness eccentricity; b and d are the length and width of the building plan with $a=b/d$ the aspect ratio of the plan; $\mathbf{B}=\mathbf{B}^T = [1 \quad 0; \quad 0 \quad 1/b]$ is a normalization matrix; \mathbf{M} and \mathbf{C} are the mass and classical damping matrix of the 2 dofs structure; $\mu_1=m_1/M_1$ is the ratio between the mass of the TM on the flexible edge and the mass of the structure; $\beta=m_2/m_1$ is the ratio between the two TMs; e_{x1} and e_{x2} are the geometric eccentricities of the TMs with respect to the CM of the building; ξ_{p1} and ξ_{p2} are the (inherent viscous) damping ratios of the TMs; ω_{p1} and ω_{p2} are the uncoupled

frequencies; and F_{TMD1} and F_{TMD2} are the non-linear components of the pendulum-forces including the MR-damper forces F_{MR1} and F_{MR2} and given by

$$F_{TMD,i} = m_i \frac{\dot{p}_i^2}{L_i^2 - p_i^2} p_i + m_i g \frac{\sqrt{L_i^2 - p_i^2}}{L_i} p_i + F_{MR(\tau, \dot{p}_i, t)} \frac{L_i^2 - p_i^2}{L_i^2} - c_i \frac{p_i^2}{L_i^2} \dot{p}_i - m_i \frac{p_i^2}{L_i^2} \mathbf{L}(\mathbf{r}_p \ddot{\mathbf{u}}_{gy} + \Phi \ddot{\eta}) \quad (2.2)$$

2.1. MR-damper constitutive model

The constitutive model used for the MR-damper is based on a simplified physical Bingham fluid model [3], i.e., with maximum force $F_{MR,max} = |F_\tau| + |F_\eta| + F_f$ and minimum force $F_{MR,min} = |F_\eta| + F_f$, where the maximum force is obtained by applying maximum current intensity to the coil and the minimum is obtained for no current intensity; F_η is the viscous force of the damper corresponding to the original viscosity of the fluid; F_f represents the frictional component of the damper force; and F_τ represents the controllable damper force, which depends on the yielding stress τ of the MR-fluid. The main advantage of the model is its simplicity in the a-priori estimation of the damper parameters, since it is physically based and does not require testing of the damper. Naturally, any model adjusted to the true measured constitutive behavior will be more accurate, but the idea in design is to develop an estimation using the nominal damper characteristics. Besides, it is computationally very efficient in carrying out the simulations. The main disadvantage of the model is that it neglects delays in changing the shear strength τ of the fluid in the damper. The viscous and controllable forces are

$$F_\eta = \left(1 + \frac{wh}{2A_p} \right) \frac{12\eta A_p^2 l_p v}{wh^3} \quad F_\tau = \left(2.07 + \frac{12\eta A_p |v|}{12\eta A_p |v| + 0.4wh^2\tau_{max}} \right) \frac{\tau_{max} A_p l_p}{h} \text{sgn}(v) \quad (2.3)$$

where η represents the viscosity of the MR-damper fluid; w is the perimeter of the gap through which the fluid passes from one chamber to the other; h is the gapsize; A_p is the section of the piston of the damper; l_p is the active polarized length of the piston [3]; and v is the velocity of the piston.

2.2. MR-damper physical control

The proposed physical controller is based on an intuitive basis, which is similar to those of a Groundhook control [4] (Figure 2). As the building departs from the at-rest configuration, the MR damper should apply maximum force to restrain the motion. This is not possible at all instants since the MR-damper is a time-varying passive device (semiaactive) and the sign of its force depends on the relative velocities of the TM and the building. Moreover as the building returns to the original at-rest configuration, it is not clear if it is convenient to push the structure back with maximum force or gradually stop this motion.

The idea of the physical controller may be better explained in reference to Figure 2, where the different states of motion of the mass and structure are schematically presented. In State 1a, when the building is displacing away from the at-rest configuration, and the relative velocity between the structure and TM is negative, the MR damper should intuitively react with maximum capacity as it tries to stop the building. However, if in State 1b the mass is swinging away from the structure, intuitively the MR should apply minimum force. In State 2, as the building is returning to its undeformed configuration, it is not apparent if it is better to push the structure back to the original position, try to stop the return, or apply an intermediate damper force. Consequently, in State 2 different controllers were evaluated using push-back forces ranging from 0% to 100%, or braking forces ranging from 0% to 100% (State 2b). For instance, in State 2a, a 50% push-back force means that in the interval between 100% and 50% of the maximum displacement of the building maximum damper force is applied; after that, the damper applies minimum force. In State 2b, 50% braking force means that maximum damper force is applied when the building displacement is smaller than half of the maximum displacement. The control just presented for a SDOF system was implemented in the real structure assuming that the monitored displacement is that of the roof of the building. The advantage of this physical control is that it requires little information on true measured building responses; it only requires the sign of the building displacement and velocity at the TM

hanging point, and the sign of the MR-damper force (or relative velocity between TM and building).

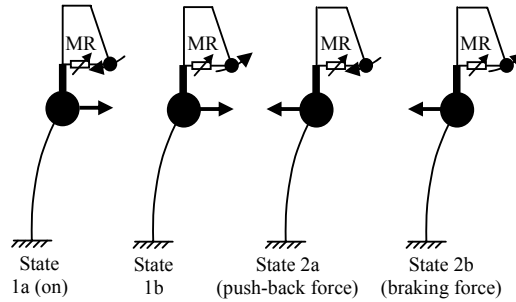


Figure 2 Schematic representation of control strategies: physical control (arrows at the building mass represent the direction of building motion at the roof and arrows on the TM represent the relative motion of the inertial mass with respect to the building)

3. BUILDING RESPONSE WITH THE TM-MR DAMPER ASSEMBLY AND SIMPLIFIED MODEL

The analysis next considers the measured vibration periods of the TMs and the nominal building periods. They were experimentally identified, $T_p=2.72s$ for the TMs, and $T_n=2.68s$ for the first Y-direction vibration mode of the building. Besides, three different values for the uncoupled torsional-to-lateral frequency ratio $\Omega=0.75, 1,$ and 1.33 and two different values of normalized eccentricity $\hat{e}_{sx}=0.82\%$ and 10% were used in this (bounded) sensitivity analysis. The first eccentricity value $\hat{e}_{sx}=0.82\%$ corresponds to that identified for the real building, and $\hat{e}_{sx}=10\%$, represents a hypothetical larger asymmetric configuration. The different control strategies just mentioned were also considered. Furthermore, each TM was equipped with one 15 ton MR-damper.

Shown in Table 1 are the displacements of the building roof and the relative displacement of the TM at the flexible and stiff edges of the building plan obtained for the different system parameters and inputs. To ease interpretation of the results, responses of the TM-MR damper assembly have been normalized with respect to the structural configuration with TMs but no MR dampers. Peak as well as RMS normalized responses were computed but only RMS-values are presented Table 1. It is apparent that the MR damper is very effective in reducing the displacement demand of the inertial mass to which it is attached; reductions are about 45% for RMS-values. In terms of RMS response reductions for the building, the effect is about 19%. Response reductions are just slightly better for the structure with larger normalized eccentricity ($\hat{e}_{sx}=10\%$) but these results are not presented in Table 1 for brevity. Normalized reductions for the building have no clear trend with Ω .

4. MR-DAMPER DESIGN AND CONSTRUCTION

A prototype of an MR-damper was designed and manufactured locally relying extensively on the comprehensive work presented by Yang [3]. The target was to achieve a 120 kN MR-damper using two coils and 3 liters of 132DG LordTM MR-fluid. The design velocity was 25 cm/s at a stroke of 10 cm, which are values calibrated for the proof-of-concept building considered. The design target was to maximize the dynamic range D of the damper, defined as the force ratio $D = (F_\tau + F_\eta + F_f) / (F_\eta + F_f) = F_{MR,max} / F_{MR,min}$. For the selected damper parameters, a maximum dynamic range is reached for passage $h=1.5mm$, resulting in a nominal dynamic range $D=15.9$, and maximum and minimum damper forces of 121kN and 7,6kN, respectively. The damper force depends on the shear strength τ of the fluid which has to be optimized. Spurious perturbations of the magnetic flux were considered in the design of the circuit[2]; such perturbations were minimized by the use of a bronze ring bearing between the head plate and the axle of the damper. Due to temperature effects of the

MR-fluid, the damper considered an expansion tank with two asymmetric check-valves.

Mechanical and electronic damper components were manufactured locally. A low carbon steel was used for metallic components to improve the magnetic flux in the damper. The two coils were finally protected by an epoxy resin. To center and align the piston within the cylinder casing, small bronze plates were welded onto the piston head. Seals used are commercial and typical for hydraulic cylinders. After assembling the damper, the MR fluid was prestressed at 90 bars as required by the results of the cavitation analysis performed [6].

Table 1 Response ratios of the 2-mode building model ($T_n = 2.68s$) with 2 TM-MR damper assemblies (physical controller with $\tau_{max} = 4.47 \text{ N/cm}^2$) versus response of building with TMs only

		RMS							Mean-RMS			Best physical controller
		S. Fel.	Mel.	Llo.	S. Fer.	El. C.	Corr.	New.	Chile	USA	Total	
$\Omega = 1.33$ $\xi_{ns} = 0.82\%$	$\hat{u}_{y,f}$	0.790	0.728	0.880	0.798	0.802	0.817	0.850	0.799	0.817	0.809	50% push back force
	$\hat{p}_{y,f}$	0.472	0.462	0.727	0.663	0.472	0.593	0.469	0.554	0.549	0.551	
	$\hat{u}_{y,s}$	0.799	0.777	0.889	0.807	0.833	0.824	0.886	0.822	0.837	0.831	
	$\hat{p}_{y,r}$	0.468	0.469	0.718	0.628	0.490	0.609	0.486	0.552	0.553	0.552	
$\Omega = 1$ $\xi_{ns} = 0.82\%$	$\hat{u}_{y,f}$	0.816	0.781	0.860	0.792	0.830	0.810	0.889	0.819	0.830	0.825	50% push back force
	$\hat{p}_{y,f}$	0.501	0.517	0.721	0.630	0.517	0.604	0.531	0.580	0.570	0.574	
	$\hat{u}_{y,s}$	0.752	0.698	0.882	0.792	0.769	0.805	0.812	0.777	0.794	0.787	
	$\hat{p}_{y,s}$	0.439	0.421	0.722	0.654	0.441	0.596	0.443	0.527	0.534	0.531	
$\Omega = 0.75$ $\xi_{ns} = 0.82\%$	$\hat{u}_{y,f}$	0.793	0.705	0.898	0.821	0.773	0.828	0.820	0.799	0.810	0.805	50% push back force
	$\hat{p}_{y,f}$	0.472	0.486	0.716	0.656	0.480	0.616	0.496	0.558	0.562	0.560	
	$\hat{u}_{y,s}$	0.793	0.786	0.873	0.788	0.850	0.814	0.893	0.817	0.836	0.828	
	$\hat{p}_{y,s}$	0.461	0.389	0.712	0.637	0.434	0.579	0.400	0.520	0.512	0.516	

5. TM-MR HYBRID SIMULATIONS

Hybrid simulations (HS) on the TM-MR damper assembly were performed at the laboratory. The simulation considered the implemented situation in the building with one MR-damper acting on the TM located along the flexible edge of the building. Because the stroke of the damper is only 10cm and it is directly connected to the TM, building input motions had to be scaled down in tests.

In implementing the HS, two controllers are required, one for the actuator to position the damper at the correct displacement and one of the damper to control its capacity. The target displacement of the TM relative to the structure (\hat{p}_y^*) is sent to the actuator controller (Figure 3). During the same integration step, the MR-damper controller sends a target voltage (V^*) to the MR-damper in order to achieve the target damper force defined by the physical controller. This force (F_m^*) is measured experimentally by a load cell, and its value fed back into the equations of motion of the structure that are running in real time in the computer. With this information, the integration moves forward from time step k to $(k + 1)$. The HS was implemented using Simulink from MATLAB. Because the displacements of the TMs in the HS are small, the building and TM behavior may be assumed linear. This fact, and the reduction of building DOFs to 20 Ritz vectors, simplifies the integration of the equations of motion. The only non-linear component is that of the MR-damper force, which is measured during the test. The linear differential equations of motion of the building with two TMs and a single MR-damper on the flexible TM may be written as:

$$\begin{bmatrix} \tilde{\mathbf{M}} + \Phi^T \mathbf{L}_p^T \mathbf{m} \mathbf{L}_p \Phi & \Phi^T \mathbf{L}_p^T \mathbf{m} \\ \mathbf{m} \mathbf{L}_p \Phi & \mathbf{m} \end{bmatrix} \begin{bmatrix} \ddot{\boldsymbol{\eta}} \\ \dot{\mathbf{p}} \end{bmatrix} + \begin{bmatrix} \tilde{\mathbf{C}} & \mathbf{0} \\ \mathbf{0} & \mathbf{c} \end{bmatrix} \begin{bmatrix} \dot{\boldsymbol{\eta}} \\ \dot{\mathbf{p}} \end{bmatrix} + \begin{bmatrix} \tilde{\mathbf{K}} & \mathbf{0} \\ \mathbf{0} & \mathbf{k} \end{bmatrix} \begin{bmatrix} \boldsymbol{\eta} \\ \mathbf{p} \end{bmatrix} + \begin{bmatrix} \mathbf{0} \\ \mathbf{F}_m \end{bmatrix} = - \begin{bmatrix} \Phi^T \mathbf{M} \mathbf{r} + \Phi^T \mathbf{L}_p^T \mathbf{m} \mathbf{L}_p \mathbf{r}_p \\ \mathbf{m} \mathbf{L}_p \mathbf{r}_p \end{bmatrix} \ddot{\mathbf{u}}_{gy} \quad (5.1)$$

where $\boldsymbol{\eta}$ and Φ are the building Ritz coordinates and vectors for the first 20 modes of a total of 78 DOFs; $\mathbf{u} = \boldsymbol{\eta} \Phi$ are the physical DOFs of the structure; $\tilde{\mathbf{M}}$, $\tilde{\mathbf{C}}$, $\tilde{\mathbf{K}}$ are the mass, damping (classic) and stiffness matrices in modal coordinates; \mathbf{r} is the influence vector for the earthquake excitation; \mathbf{u}_{gy} is the ground acceleration in the Y-direction; \mathbf{p} are the displacements of the TMs relative to the roof of the building; \mathbf{L}_p is the kinematic transformation matrix between the degrees of freedom \mathbf{u} and the building displacements at the location of the TMs; \mathbf{m} , \mathbf{c} and \mathbf{k} are the mass, viscous damping, and stiffness matrices of the linear TMs; \mathbf{r}_p is the input influence vector of the TM for earthquake excitations; and $\mathbf{F}_m = [F_m \ 0 \ 0 \ 0]^T$ is the vector with the measured damper force F_m . Finally, to carry out the simulations, the differential equations of motion of the structure are expressed in the state-space format (Figure 3). The proposed physical controller and the well-known LQR controller were implemented for the TM-MR damper assembly. Experimental results showed that the performances observed for the two controllers are quite similar, and hence, results are presented only for the physical one.

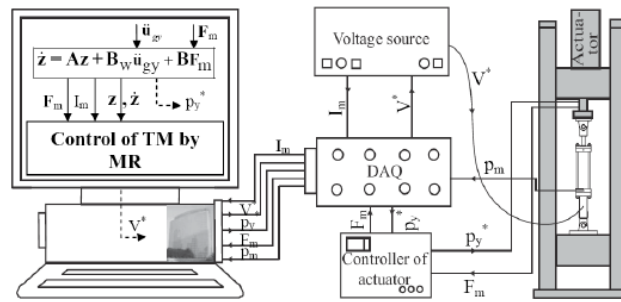


Figure 3 Schematic view and information flow of HS test

Shown in Figure 4 is a comparison of the analytical and HS building response with the TM-MR damper assembly relative to the structure without TMs (triangle pointing upward) and the following analysis cases: (i) HS of the TMs with one MR-damper on the flexible edge of the building (circle); (ii) analytical response of the building with TMs but without dampers (inverted triangle); (iii) analytical response of the building with TMs and one optimal viscous damper on the flexible edge (diamond); and (iv) analytical response of the structure with MRD (curves). Peak and RMS values for the Chilean and US records are presented; identical earthquakes use identical markers. The abscissa in the Figure indicates the different levels of maximum shear strength τ_{max} in the fluid (case (iv)), which represents different peak electric current intensity levels; the ordinates indicate the peak or RMS responses along the flexible edge. For most cases of the peak, and RMS cases, the performance of the structure with the TM-MR damper assembly is better than the response of the structure without dampers. Ground motion input cases where the TMs alone work well, usually correspond to cases in which the MR-damper downgrades the performance of the system. TMs passively controlled by ideal frictionless viscous dampers also show an improved performance relative to the case with just TMs. In general, by using the TM-MR damper assembly, the improvement in building response is significant. However, analytical reductions are larger than the ones obtained by HS, the reason being a 30V voltage source used in laboratory tests that impeded quick changes of the MR damper force.

6. BUILDING IMPLEMENTATION OF THE MR-DAMPER

Shown in Figure 5 is the building setup used for testing the TM-MR damper assembly—the building setup is similar to the one used for HS. The computer controls the MR-damper force by controlling the current intensity sent through a controllable 30V power source. The implementation of the physical controller in the building

considered just the sign of the building displacement and velocity at the location of the TM, and the sign of the MR-damper force. The sign of the damper force is indirectly obtained from the sign of the relative velocity between the TM and the building at the location of the mass. This relative velocity between the TM and the building was obtained by taking the first derivative of the measured relative displacement. Building displacements were determined by integrating the measured building velocity.

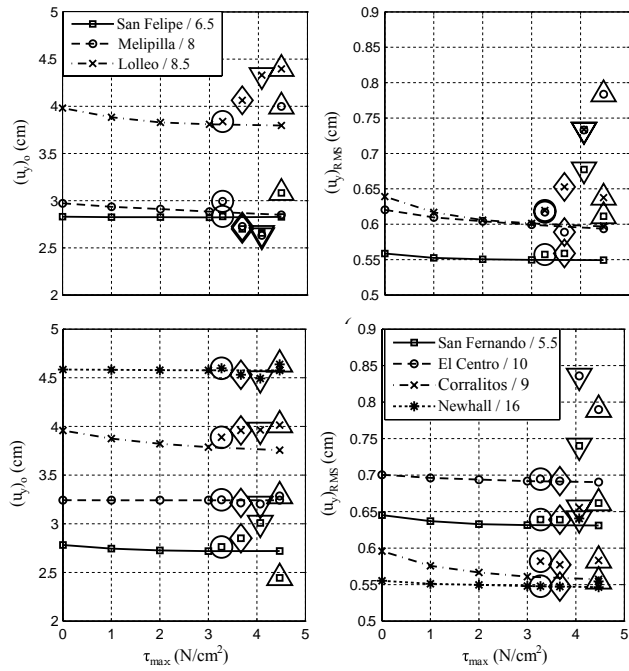


Figure 4 Comparison of theoretical versus HS results of peak and RMS building displacements of the flexible edge of the building: (a) scaled Chilean records, and (b) scaled US records

In order to check the TM-MR damper assembly and the control strategy, pull-back tests were performed on the TM. Figure 6 shows that the response of the 160 ton mass may be controlled in one cycle by the proposed physical controller with only one coil active, which results in a maximum damper force of about 80 kN. By controlling the TM by the MR-damper, the peak Y-displacement of the TM is reduced by about 26% (79% RMS). This shows that the capacity of the damper is adequate for the application developed. This Figure also shows that the displacements of the building may be reduced by the use of an MR damper—this is relevant in a flexible building like this one since additional damage may eventually occur in free vibration after the ground motion has finished. In this case, the peak displacement of the building is reduced by 22% (63% RMS). Comparing the controlled MR-damper with the passive off case, reductions of about 4% and 14 % for peak and RMS values are obtained in the TM displacements. Peak and RMS building displacements are reduced by 3% and 20%, respectively. This proves the functionality of the implemented physical controller.

7. CONCLUSION

This investigation dealt with the simulation, design, construction, testing, and implementation of a prototype 150kN MR damper in the first tall free-plan building in Santiago, Chile, that has been equipped with two 160 ton TMs. Average results for this particular structure show that the improvement in RMS displacement reduction due to the MR damper, relative to the structure with TMs only, ranges between 12% and 24%. These response reductions and other model assumptions were confirmed at the experimental phase through harmonic and HS tests for the structure subjected to a suite of far- and near-field ground excitations. The Bingham constitutive model used for the MR-damper and the proposed physical controller of the TM-MR damper assembly are adequate, robust, and simple to implement in practice. Pull-back tests of the TM-MR damper

assembly in the building demonstrate that this system is capable of controlling the lateral response of the 21-story structure with maximum damper capacity of the order of 150kN. Besides, given the simplicity of the controller proposed, real-time control is achievable with simple components.

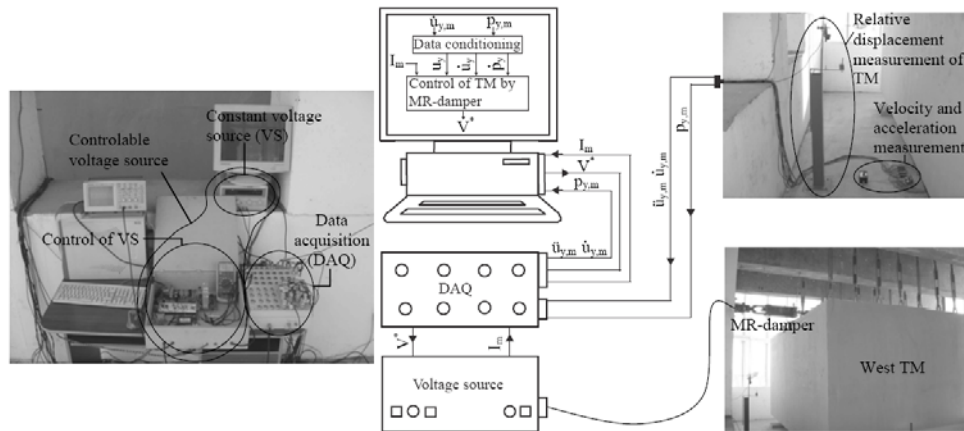


Figure 5 MR-damper implementation in the building

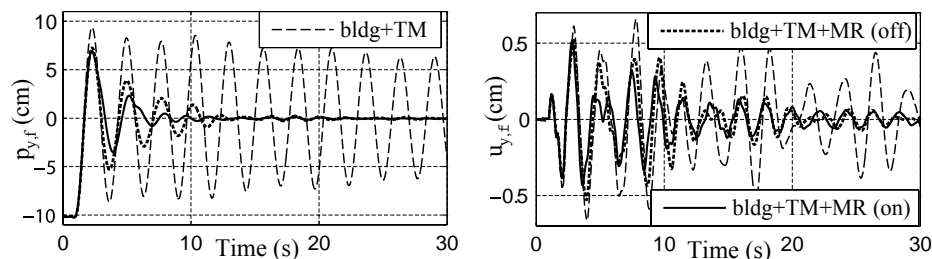


Figure 6 Measured TM and flexible-edge displacements from typical pull-back test and different damper conditions

ACKNOWLEDGEMENTS

This research has been funded by the Chilean National Fund for Research and Technology, Fondecyt, through Grant N° 1085282.

REFERENCES

1. Zemp R., de la Llera J.C. (Submitted for publication July 2008). Tall building vibration control using a TM-MR damper assembly: analytical results. *Earthquake Engineering and Structural Dynamics*.
2. Zemp R., de la Llera J.C. (Submitted for publication July 2008). Tall building vibration control using a TM-MR damper assembly: experimental results and implementation. *Earthquake Engineering and Structural Dynamics*.
3. Yang G. (2001). Large-Scale Magnetorheological Fluid Damper for Vibration Mitigation: Modeling, Testing and Control. *Ph.D. Dissertation, Department of Civil Engineering and Geological Sciences, Notre Dame, Indiana, USA*.
4. Setareh M., (2001). Application of semi-active tuned mass dampers. *Earthquake Engineering and Structural Dynamics*.
5. Lin P. Y., Chung L. L., Loh C. H. (2005) Semiactive Control of Building Structures with Semiactive Tuned Mass Damper. *Computer-Aided Civil and Infrastructure Engineering* **20**: 1, 35-51.
6. Zemp R. (2008). Tall building vibration control using a TM-MR damper assembly. Master Thesis, Department of Structural and Geotechnical Engineering, Pontificia Universidad Católica de Chile.